

**Polyoxometalate-templated lanthanide–organic hybrid layers based on 6<sup>3</sup>-honeycomb-like 2D nets†**

Xiu-Li Hao, Ming-Fa Luo, Wei Yao, Yang-Guang Li,\* Yong-Hui Wang\* and En-Bo Wang

Received 25th January 2011, Accepted 29th March 2011

DOI: 10.1039/c1dt10139k

The reaction of a double-betaine-containing ligand with  $\text{LnPMo}_{12}\text{O}_{40}\cdot n\text{H}_2\text{O}$  ( $\text{Ln} = \text{Dy, Tb and Er}$ ) led to the isolation of new polyoxometalate-templated lanthanide–organic hybrid layers with the molecular formula  $[\text{Ln}(\text{L})_{1.5}(\text{H}_2\text{O})_5][\text{PMo}_{12}\text{O}_{40}]\cdot 1.5\text{CH}_3\text{CN}\cdot 2\text{H}_2\text{O}$  ( $\text{Ln} = \text{Dy}$  (**1**),  $\text{Tb}$  (**2**) and  $\text{Er}$  (**3**);  $\text{L} = 1,4$ -bis(pyridinil-4-carboxylato)-1,4-dimethylbenzene). All compounds were characterized by elemental analyses, TG analyses, IR and the single-crystal X-ray diffraction. Compounds **1–3** are isostructural and possess a 2D undulating cationic network  $[\text{Ln}(\text{L})_{1.5}(\text{H}_2\text{O})_5]^{3n+}$  with the honeycomb-like cavities. Interestingly, the interval 2D networks are further connected by the H-bonds to form a 3D supramolecular framework. Moreover, two of such identical supramolecular frameworks are 2-fold interpenetrated with each other and encapsulate the  $\alpha$ -Keggin-type  $[\text{PMo}_{12}\text{O}_{40}]^{3-}$  anionic templates and the solvent molecules. These composite compounds display both luminescent properties (induced by organic ligands and/or lanthanide ions) and electrocatalytic activities towards the reduction of nitrite.

**Introduction**

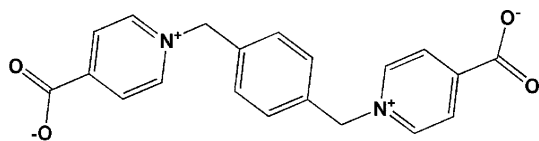
Metal–organic coordination polymers with cavities, pores and/or channels are of great interest due to not only their chemical and structural diversities but also their promising applications in catalysis, gas storage, separation, and molecular recognition.<sup>1</sup> During the synthesis, an important strategy is the use of various templates to assemble such type of hybrid compounds.<sup>2,3</sup> In recent years, many anions have been employed as templates.<sup>3</sup> In this aspect, polyoxometalates (POMs), as one type of unique nano-sized metal-oxo clusters, can be the outstanding anionic templates due to their controllable shape, size, high negative charges and abundant chemical combinations with multiple functionalities.<sup>4–9</sup> In this sub-family, most POM-templated metal–organic networks or frameworks are constructed by the transition metal (TM) ions and various neutral organic N-donor ligands.<sup>5–7</sup> In comparison, the analogues based on lanthanide–organic hybrid moieties and POM templates have rarely been reported<sup>9</sup> and become a currently new research focus especially considering that the lanthanide complexes may endow new POM-based composite materials with “value-added” functionalities such as luminescent, magnetic, and/or catalytic properties.<sup>10</sup> However, several problems have arisen during the synthesis of such compounds: (i) the oxophilic

lanthanide ions usually possess high reactivity with oxygen-enriched POMs, which always leads to precipitate instead of crystallization;<sup>11</sup> (ii) lanthanide ions exhibit relatively low coordination ability with many N-donor linking ligands, especially in the acidic media; (iii) When using the anionic O-donor ligands, for example, the multi-carboxylate-containing ligands, the reaction competition between polyoxoanions and anionic organic O-donor ligands with lanthanide ions can not be easily avoided and often leads to unexpected results;<sup>12</sup> (iv) furthermore, using neutral O-donor ligands might provide a solution for the above problem (iii) but such neutral O-donor linkers remains far unexplored in contrast to the neutral N-donor ligands.<sup>9a</sup> Therefore, the design and synthesis of new POM-templated lanthanide–organic networks or frameworks is still a great challenge.

Based on aforementioned considerations, the double betaine-containing ligands may be one of suitable organic linkers for the assembly of such POM-templated lanthanide–organic hybrid compounds. The betaine-type ligands usually contain both anionic carboxylate groups and cationic amino groups, exhibiting the zwitterionic properties and overall charge neutrality.<sup>13</sup> In comparison to the anionic double-carboxylate-containing ligands, the double-betaine-type ligands may not only keep the versatile coordination modes of carboxylate groups but also provide a new type of neutral O-donor linkers.<sup>13</sup> So far, such type of O-donor ligands have never been used to construct POM-based metal–organic hybrid compounds. Herein, we synthesized a flexible double-betaine-containing ligand, that is, the 1,4-bis(pyridinil-4-carboxylato)-1,4-dimethylbenzene (**L**) (see Scheme 1). The slow reaction of **L** with  $\text{LnPMo}_{12}\text{O}_{40}\cdot n\text{H}_2\text{O}$  ( $\text{Ln} = \text{Dy, Tb or Er}$ ) resulted in the isolation of three new POM-templated lanthanide-organic 2D networks with the molecular formula

Key Laboratory of Polyoxometalate Science of Ministry of Education, Faculty of Chemistry, Northeast Normal University, Changchun 130024, P. R. China. E-mail: liyg658@nenu.edu.cn, wangyh319@nenu.edu.cn; Fax: +86 43185098787; Tel: +86 43185099193

† Electronic supplementary information (ESI) available: Additional structural figures, IR, TG and CV. CCDC reference numbers 808504, 808505 and 808506 for compounds **1–3**. For ESI and crystallographic data in CIF or other electronic format see DOI: 10.1039/c1dt10139k



**Scheme 1** The structure of double-betaine-containing ligand (**L** = 1,4-bis(pyridinil-4-carboxylato)-1,4-dimethylbenzene).

$[\text{Ln}(\text{L})_{1.5}(\text{H}_2\text{O})_5][\text{PMo}_{12}\text{O}_{40}] \cdot 1.5\text{CH}_3\text{CN} \cdot 2\text{H}_2\text{O}$  ( $\text{Ln} = \text{Dy}$  (**1**),  $\text{Tb}$  (**2**) and  $\text{Er}$  (**3**)). The double-betaine-type ligand as neutral linkers is firstly introduced into the POM-based lanthanide-organic hybrid materials. The luminescent and electrocatalytic properties of these composite compounds were investigated.

## Experimental

### Materials and methods

All chemicals and organic solvents used for synthesis were of reagent grade without further purification. The lanthanide chlorides  $\text{LnCl}_3 \cdot 6\text{H}_2\text{O}$  ( $\text{Ln} = \text{Dy}$ ,  $\text{Tb}$ ,  $\text{Er}$ ) were prepared by dissolving  $\text{Ln}_2\text{O}_3$  (99.9%) in hydrochloric acid, followed by concentration and crystallization. The  $\alpha\text{-H}_3\text{PMo}_{12}\text{O}_{40} \cdot 14\text{H}_2\text{O}^{14}$  and  $\text{LnPMo}_{12}\text{O}_{40} \cdot n\text{H}_2\text{O}$  ( $\text{Ln} = \text{Dy}$ ,  $\text{Tb}$ ,  $\text{Er}$ )<sup>9a</sup> were prepared according to the literature methods. Elemental analyses (C, H and N) were analyzed on a Perkin–Elmer 2400 CHN elemental analyzer. The FT-IR spectra were performed on a Mattson Alpha-Centauri spectrometer with KBr pellets in the range of 4000–400  $\text{cm}^{-1}$ . TG analyses were carried out on a Pyris Diamond TG instrument in flowing  $\text{N}_2$  with a heating rate of 10  $^\circ\text{C min}^{-1}$ . Electrochemical experiments were measured on a BAS Epsilon Analyzer in a three-electrode cell: glassy carbon electrode (GCE, diameter 3 mm) as a working electrode, platinum wire as a counter electrode, and  $\text{Hg}/\text{HgCl}$  as a reference electrode. The solid-state emission/excitation spectra of compounds **1–3** were measured on a SPEX FL-2T2 spectrofluorimeter equipped with a 450 W xenon lamp as the excitation source.

### Synthesis

**1,4-Bis(pyridinil-4-carboxylato)-1,4-dimethylbenzene (L).** The flexible double betaine ligand was prepared in a modified way similar to that in the literature.<sup>15</sup> 1,4-Bis-chloromethyl-benzene (1.75 g, 10 mmol) (instead of 1,4-bis-bromomethyl-benzene) was dissolved in the acetone solution of ethyl isonicotinate (3.1 mL, 20 mmol). The mixture was refluxed and filtered to give a white precipitate, which was hydrolyzed by dilute hydrochloric acid (5%, 50 mL). Then, the chloride ions were removed by the fresh silver(I) oxide (prepared by the reaction of  $\text{AgNO}_3$  and  $\text{NaOH}$  in aqueous solution) and the white powder of **L** were obtained. Anal. calcd (%) for **L** ( $\text{C}_{20}\text{H}_{16}\text{N}_2\text{O}_4$ ): C 68.96, H 4.63, N 8.04. Found (%): C 68.82, H 4.68, N 8.13. IR (KBr,  $\text{cm}^{-1}$ ): 3112(w), 3035(w), 2997(w), 1633(s), 1567(m), 1519(m), 1458(m), 1432(m), 1356(s), 781(s), 756(s); 693(s).

**$[\text{Dy}(\text{L})_{1.5}(\text{H}_2\text{O})_5][\text{PMo}_{12}\text{O}_{40}] \cdot 1.5\text{CH}_3\text{CN} \cdot 2\text{H}_2\text{O}$  (**1**).** A solvent mixture (10 mL) of acetonitrile and water ( $v/v = 3:2$ ) was used as a buffer layer and very carefully layered over an aqueous solution (4 mL) of **L** ligand (35 mg, 0.1 mmol) in a long and thin tube. Then,  $\text{DyPMo}_{12}\text{O}_{40} \cdot n\text{H}_2\text{O}$  (67 mg,  $\sim 0.033$  mmol) in 4 mL mixture

of acetonitrile and water ( $v/v = 3:1$ ) was slowly layered over the buffer layer. The tube was sealed and left undisturbed at room temperature. After one month, the yellow block crystals were isolated in the buffer layer and collected by filtration (Yield: 55% based on Mo). Anal. calcd for  $\text{C}_{33}\text{H}_{42.5}\text{N}_{4.5}\text{O}_{53}\text{PMo}_{12}\text{Dy}$ : C 14.64, H 1.56, N 2.37. Found: C 14.69, H 1.58, N 2.34. Selected IR (KBr pellet,  $\text{cm}^{-1}$ ): 3118(w), 3059(w), 1634(m), 1563(m), 1458(w), 1384(m), 1063(s), 957(s), 878(m), 800(s), 687(w).

**$[\text{Tb}(\text{L})_{1.5}(\text{H}_2\text{O})_5][\text{PMo}_{12}\text{O}_{40}] \cdot 1.5\text{CH}_3\text{CN} \cdot 2\text{H}_2\text{O}$  (**2**).** Compound **2** was prepared in the same way as **1** except that  $\text{TbPMo}_{12}\text{O}_{40} \cdot n\text{H}_2\text{O}$  (0.033 mmol) was used instead of  $\text{DyPMo}_{12}\text{O}_{40} \cdot n\text{H}_2\text{O}$ . After one month, the yellow block crystals were isolated and collected by filtration (Yield: 50% based on Mo). Anal. calcd for  $\text{C}_{33}\text{H}_{42.5}\text{N}_{4.5}\text{O}_{53}\text{PMo}_{12}\text{Tb}$ : C 14.68, H 1.61, N 2.36. Found: C 14.72, H 1.58, N 2.34. Selected IR (KBr pellet,  $\text{cm}^{-1}$ ): 3102(w), 3060(w), 1635(m), 1565(m), 1457(w), 1364(s), 1063(s), 958(s), 871(m), 771(s), 654(w).

**$[\text{Er}(\text{L})_{1.5}(\text{H}_2\text{O})_5][\text{PMo}_{12}\text{O}_{40}] \cdot 1.5\text{CH}_3\text{CN} \cdot 2\text{H}_2\text{O}$  (**3**).** Compound **3** was prepared in the same way as **1** except that  $\text{ErPMo}_{12}\text{O}_{40} \cdot n\text{H}_2\text{O}$  (0.033 mmol) was used instead. After one month, the yellow block crystals were isolated and collected by filtration (Yield: 62% based on Mo). Anal. calcd for  $\text{C}_{33}\text{H}_{42.5}\text{N}_{4.5}\text{O}_{53}\text{PMo}_{12}\text{Er}$ : C 14.65, H 1.59, N 2.31. Found: C 14.67, H 1.57, N 2.33. Selected IR (KBr pellet,  $\text{cm}^{-1}$ ): 3118(w), 3058(w), 1636(m), 1568(m), 1459(w), 1377(m), 1062(s), 956(s), 878(m), 799(s), 686(w).

### X-Ray crystallography

The crystallographic data of three compounds were collected at 150 K on the Rigaku R-axis Rapid IP diffractometer using graphite monochromatic  $\text{Mo-K}\alpha$  radiation ( $\lambda = 0.71073 \text{ \AA}$ ) and IP techniques. A multi-scan absorption correction as applied. The crystal data of **1**, **2** and **3** were solved by the direct method and refined by a full-matrix least-squares method on  $F^2$  using the SHELXTL-97 crystallographic software package.<sup>16</sup> All non-H atoms were refined anisotropically except the disordered solvent water molecules. H atoms on the C atoms were fixed in calculated positions. H atoms on the coordinated water molecules were found from the difference Fourier maps and fixed in reasonable positions. However, the H atoms on the lattice water molecules cannot be found from the residual peaks but were directly included in the final molecular formula. The detailed crystal data and structure refinement for **1–3** are given in Table 1. Selected bond lengths and angles of **1–3** are listed in Table S1–S3, respectively.†

## Results and discussion

### Synthesis

During the preparation of compounds **1**, **2** and **3**, the starting materials  $\text{LnPMo}_{12}\text{O}_{40} \cdot n\text{H}_2\text{O}$  ( $\text{Ln} = \text{Dy}$ ,  $\text{Tb}$  or  $\text{Er}$ ) can not be directly mixed with **L** ligand, otherwise plenty of precipitates would be immediately isolated from the solution. These precipitates exhibit very low solubility in water and common organic solvents such as acetonitrile, methanol and ethanol. Furthermore, the **L** ligand will decompose in aqueous solutions if the reaction temperature is higher than 80  $^\circ\text{C}$ . Hence, the hydrothermal technique can not be employed in such a reaction system. In this case, the slow

**Table 1** Crystal data and structure refinement for **1–3**

Compounds	<b>1</b>	<b>2</b>	<b>3</b>
Formula	C <sub>33</sub> H <sub>42.5</sub> N <sub>4.5</sub> O <sub>53</sub> PMo <sub>12</sub> Dy	C <sub>33</sub> H <sub>42.5</sub> N <sub>4.5</sub> O <sub>53</sub> PMo <sub>12</sub> Tb	C <sub>33</sub> H <sub>42.5</sub> N <sub>4.5</sub> O <sub>53</sub> PMo <sub>12</sub> Er
<i>M<sub>r</sub></i>	2694.97	2691.39	2699.73
<i>T</i> /K	150(2)	150(2)	150(2)
Crystal system	Triclinic	Triclinic	Triclinic
Space group	<i>P</i> $\bar{1}$	<i>P</i> $\bar{1}$	<i>P</i> $\bar{1}$
<i>a</i> /Å	11.900(2)	11.921(2)	11.921(2)
<i>b</i> /Å	15.167(3)	15.142(3)	15.166(3)
<i>c</i> /Å	21.059(4)	21.053(4)	21.020(4)
$\alpha$ /°	100.61(3)	100.51(3)	100.49(3)
$\beta$ /°	90.83(3)	90.91(3)	90.79(3)
$\gamma$ /°	102.67(3)	102.78(3)	102.89(3)
<i>V</i> /Å <sup>3</sup>	3639.0(12)	3637.6(12)	3636.7(12)
<i>Z</i>	2	2	2
$\mu$ /mm <sup>-1</sup>	3.134	3.080	3.263
<i>F</i> (000)	2562	2560	2566
Reflections	28 656	28 122	28 272
Independent Reflections ( <i>R</i> <sub>int</sub> )	12 732 (0.0623)	12 589 (0.0962)	12 635 (0.0711)
GOF <sup>a</sup>	1.032	1.035	1.007
<i>R</i> <sub>1</sub> [ <i>I</i> > 2σ( <i>I</i> )] <sup>a</sup>	0.0595	0.0718	0.0674
w <i>R</i> <sub>2</sub> (all data) <sup>b</sup>	0.1662	0.1829	0.1895
Δρ <sub>max/min</sub> /e Å <sup>-3</sup>	1.163/−1.521	1.103/−1.291	1.195/−0.970

<sup>a</sup>  $R_1 = \sum |F_o| - |F_c| / \sum |F_o|$ . <sup>b</sup>  $wR_2 = \sum [w(F_o^2 - F_c^2)^2] / \sum [w(F_o^2)^2]^{1/2}$ .

diffusion method is employed for the assembly of new POM-templated lanthanide–organic networks. As to such a method, the density and polarity of the solvent media play an important role for the preparation of single crystals with good qualities. In our experiments, water is chosen as the heavy solvent to dissolve the organic ligands in the bottom layer of the tube. The density of the middle buffer layer is adjusted by the mixture of CH<sub>3</sub>CN : H<sub>2</sub>O (*v/v* = 3 : 2). The top LnPMo<sub>12</sub>O<sub>40</sub> salts are dissolved in the solvent mixture of CH<sub>3</sub>CN : H<sub>2</sub>O (*v/v* = 3 : 1). The increase of the amount of CH<sub>3</sub>CN from bottom to top can keep the three layers well separated in the tube and maintain a relatively slow diffusion speed. It is worth emphasizing that the middle buffer layer should keep a little higher so as to avoid the quick reaction between top LnPMo<sub>12</sub>O<sub>40</sub> and bottom organic ligands.

### Crystal structures

Single-crystal X-ray diffraction analyses show that compounds **1–3** are isostructural, thus, **1** is described here as the representative example. Compound **1** crystallizes in the triclinic space group *P* $\bar{1}$ , and the basic structural unit consists of the cationic complex moiety [Dy(L)<sub>1.5</sub>(H<sub>2</sub>O)<sub>5</sub>]<sup>3+</sup>, the Keggin-type polyoxoanion [PMo<sub>12</sub>O<sub>40</sub>]<sup>3-</sup>, one and a half crystalline acetonitrile molecules, and three water molecules (ESI, Fig. S1–S3).<sup>†</sup> In **1**, the guest polyoxoanion [PMo<sub>12</sub>O<sub>40</sub>]<sup>3-</sup> shows the typical α-Keggin type structural feature with the approximate *T<sub>d</sub>* symmetry (see Fig. S1).<sup>†</sup> In the cationic dysprosium–organic layer of **1**, each Dy<sup>3+</sup> ion coordinates with three oxygen atoms derived from the carboxylate groups of three different L ligands and five coordinated water molecules and exhibits a distorted square anti-prismatic coordination geometry (Fig. 1 and Fig. S4).<sup>†</sup> The bond distances of Dy–O are in the range of 2.237(1)–2.389(1) Å. Furthermore, all L ligands adopt a *trans*-configuration and each carboxylate group on the L ligand displays a monodentate coordination mode with one Dy center. (Fig. 1). The Dy ⋯ Dy separation across the L ligand is *ca.* 19.87 Å. Based on above coordination mode, the Dy centers are linked by the L

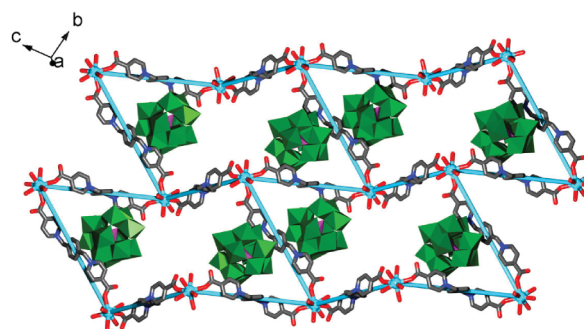


**Fig. 1** The structure of cationic 2D lanthanide–organic network in **1**. Each honeycomb-like cavity encapsulates two Keggin-type POM templates. The blue lines show that such a 2D network exhibits a 6<sup>3</sup>-hcb net topology. The H atoms and solvent molecules are omitted for clarity.

ligands to form an undulating 2D network with honeycomb-like cavities. From a topological perspective, each Dy center can be viewed as a 3-connected node and the L ligands are linear linkers. Thus, such a 2D network can be regarded as a honeycomb-like 6<sup>3</sup>-hcb net (Fig. 1 and Fig. S4).<sup>†</sup> Interestingly, each six-membered ring in the 2D net is large enough to contain two Keggin-type polyoxoanion templates, which has rarely been observed.<sup>7a</sup>

In the packing arrangement, all of these identical 2D layers are parallel with each other, and two adjacent nets have no obvious intermolecular interactions. However, the typical hydrogen bonds occur between the coordination water molecules (O5w) and the carboxylate groups (O42) from the interval networks (See Fig. 2a). The typical H-bond length of O5w–H5aw ⋯ O42 is 2.486 Å. The interval 2D networks are then hydrogen-bonded with each other to form a 3D supramolecular framework (see Fig. 2b–c and Fig. S5).<sup>†</sup> More interestingly, two independent but identical 3D supramolecular frameworks are entangled with each other in a 2-fold interpenetration mode. (Fig. 2d and Fig. S5).<sup>†</sup> The large voids of the 3D supramolecular framework are occupied by the

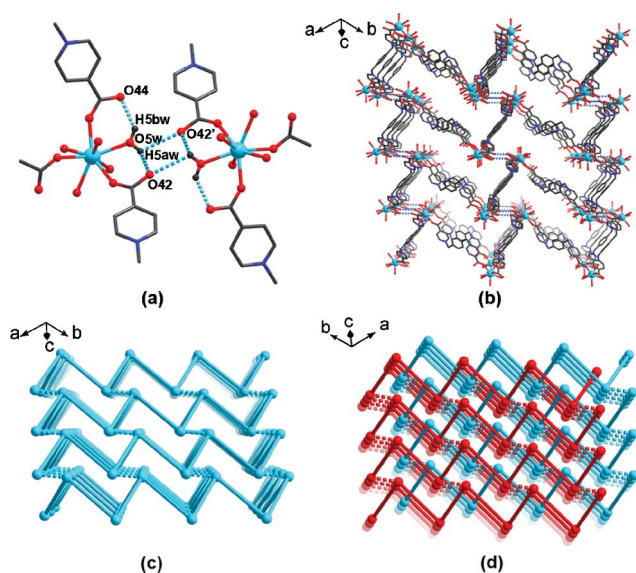


**Fig. 2** (a) The typical hydrogen bonding interactions between two interval layers in **1** (O5w–H5bw...O44 1.966 Å; O5w–H5aw...O42 2.126 Å, O5w–H5aw...O42' 2.486 Å with the symmetry operation:  $-x, -y + 2, -z + 1$ ). (b) Interval lanthanide-organic networks in **1** are linked by the H-bonds to form a 3D supramolecular framework. (c) Schematic views of 3D supramolecular framework in **1**. (d) Schematic view of the entangled 3D supramolecular framework in a 2-fold interpenetration mode.

Keggin-type POM templates and solvent MeCN and water molecules (Fig. 3 and Fig. S6).<sup>†</sup> To our knowledge, compounds **1–3** represent the first POM-templated lanthanide-organic hybrids exhibiting the entangled 3D supramolecular frameworks.

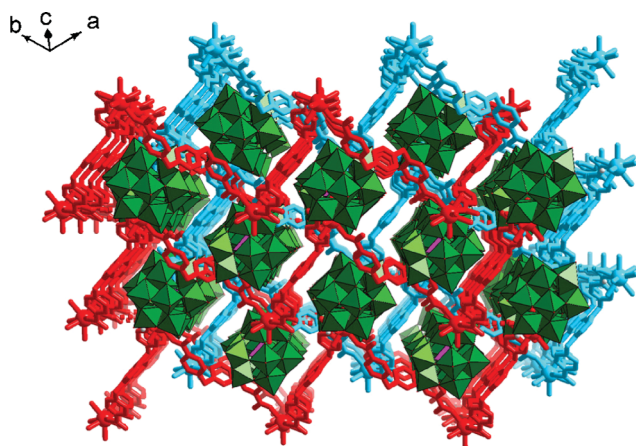


**Fig. 3** Structural view of the host lanthanide-organic supramolecular framework encapsulating the POM templates in **1**. The H atoms and solvent molecules are omitted for clarity.

### Electrochemical and electrocatalytic properties

Polyoxometalates usually undergo reversible multi-electron redox processes, especially the Keggin-type polyoxomolybdates represent one of good models for the electrochemical investigation.<sup>17</sup> Moreover, it is also interesting to explore the electrochemical behaviours and changes of such Keggin-type polyoxomolybdates when these multi-electron carriers are encapsulated into various

cationic metal-organic networks.<sup>5d–f,6,7</sup> Herein, the electrochemical behaviours of compounds **1–3** were studied with the **1**-, **2**- and **3**-modified carbon paste electrodes (**1**-, **2**- and **3**-CPEs) since these composite compounds are dissolvable in water and common organic solvents.<sup>17,18</sup> The cyclic voltammetry (CV) measurements of **1**-, **2**- and **3**-CPEs at different scan rates were recorded in the potential range from +700 to –200 mV in 1 M H<sub>2</sub>SO<sub>4</sub> (Fig. 4a and Fig. S8b–S9b).<sup>†</sup> The CV behaviours of three samples are similar and only that of **1**-CPE is described here. As shown in Fig. 4a, three pairs of reversible redox peaks of **1**-CPE appear in the range of +700 to –200 mV, and the mean peak potentials ( $E_{1/2} = (E_{cp} + E_{ap})/2$ ) are 400, 252 and –15 mV with the scan rate of 100 mV s<sup>-1</sup> (Fig. S7). The reversible peaks I–I', II–II', and III–III' correspond to a two-, four-, and six-electron redox process of [PMO<sub>12</sub>O<sub>40</sub>]<sup>3-</sup> unit, respectively, which is similar to the reported Keggin-type [PMO<sub>12</sub>O<sub>40</sub>]<sup>3-</sup> species.<sup>19</sup> The peak currents are proportional to the scan rate up to 200 mV s<sup>-1</sup>, indicating that the redox process of **1**-CPE is surface-controlled (Fig. 4a insert).

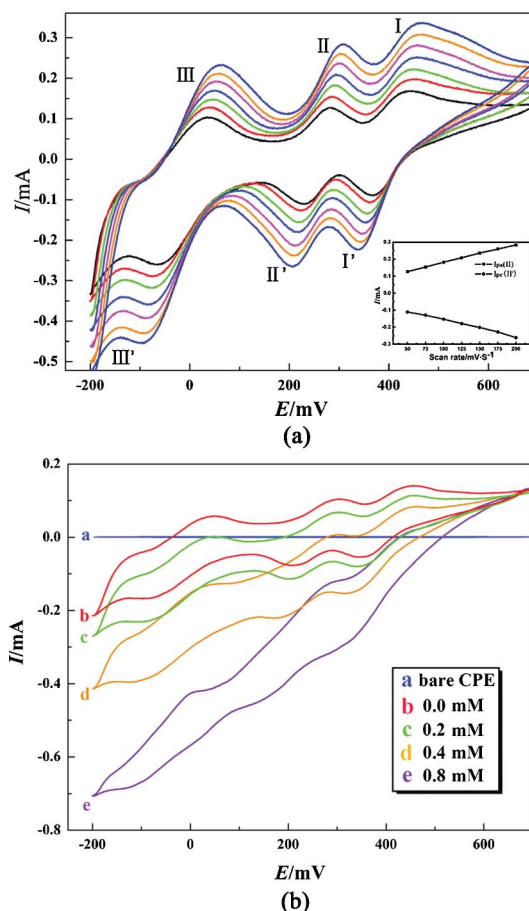


**Fig. 4** (a) The cyclic voltammograms (CV) of **1**-CPE in 1 M H<sub>2</sub>SO<sub>4</sub> at different scan rates (from inner to outer: 50, 75, 100, 125, 150, 175 and 200 mV s<sup>-1</sup>). The inset shows plots of the dependence of anodic peak and cathodic peak (II–II') current on scan rates; (b) CVs of the **1**-CPE in 1 M H<sub>2</sub>SO<sub>4</sub> solution containing 0.0–0.8 mM KNO<sub>2</sub> and a bare CPE in 0.50 mM KNO<sub>2</sub> + 1 M H<sub>2</sub>SO<sub>4</sub> solution.

In the electrochemical studies of POM-based hybrid materials, one of the most interesting works is to discover the potential electrocatalytic properties of such compounds since many of them

can be used as good electrocatalysts for the reduction of polluting substances in aqueous solutions such as nitrite, hydrogen peroxide and iodate.<sup>5d,6,7,20</sup> In contrast to the CPEs modified by the soluble alkali salts of POMs, the POM-templated metal-organic hybrid materials may both avoid the partial loss of POMs in aqueous and/or organic media (that is, stabilize the POMs due to their low solubility) and keep the electrocatalytic activity of POMs, which thus represent one type of ideal electrocatalysts. Therefore, the electrocatalytic properties of compounds **1**–**3** modified CPEs were further investigated towards the reduction of nitrite in an aqueous solution. The CV for the electrocatalytic reduction of nitrite at **1**-CPE in a 1 M H<sub>2</sub>SO<sub>4</sub> aqueous solution is shown in Fig. 4b. On addition of NO<sub>2</sub><sup>-</sup>, all three reduction peak currents increased while the corresponding oxidation peak currents dramatically decreased, indicating that nitrite was reduced by all three reduced polyoxoanion species.<sup>17</sup> It is noteworthy that the third reduced species shows the best electrocatalytic activity, which suggests that the increase of reduction extent of the Keggin anion species may enhance their catalytic activities. In contrast, the reduction of nitrite at a bare electrode generally requires a large overpotential and no obvious response was observed in the range +700 to -200 mV on a bare CPE (Fig. 4b). It is also worth mentioning that the peak currents of **1**-CPE maintain almost unchanged over 100 cycles at a scan rate of 100 mV s<sup>-1</sup> when the potential range is kept between +700 and -200 mV, revealing that **1**-CPE possesses a relatively high stability.<sup>20</sup> Similar behaviours were also observed for **2**- and **3**-CPEs (Fig. S8d–S9d).†

### Luminescent properties

The luminescent properties of compounds **1**–**3** have also been explored, considering that both lanthanide ions and the organic ligands may induce the luminescent behaviours. Actually, two kinds of emission regions were observed for compound **2**, and only one emission region is found for **1** and **3** (Fig. 5). The first emission region of compound **2** was obtained with an excitation wavelength of 260 nm and involves a low-intensity emission band at 494 nm and a high-intensity emission peak at 559 nm, corresponding to the <sup>5</sup>D<sub>4</sub> → <sup>7</sup>F<sub>6</sub> and <sup>5</sup>D<sub>4</sub> → <sup>7</sup>F<sub>5</sub> transitions of Tb<sup>3+</sup> ion, respectively. (Fig. 5b).<sup>21</sup> Moreover, another intense emission peak of compound **2** is located at 423 nm upon excitation at 368 nm (Fig. 5a) and can be assigned to organic ligand-based emission according to the luminescence spectrum of the free L ligand (Fig. 5a). This emission band can be ascribed to a π–π\* or π–n ligand-centered electronic transition within the aromatic systems of the L ligand.<sup>22</sup> Furthermore, the emission peak positions at ca. 423 nm for compounds **1** and **3** are similar to that of **2** (Fig. 5a), but the characteristic emission bands of Dy<sup>3+</sup> and Er<sup>3+</sup> ions cannot be observed. It is presumed that the aqua ligands on these lanthanide ions may lead to the fluorescence quenching.<sup>23</sup> The above observations suggest that these POM-based composite materials of **1**–**3** may be suitable candidates for potential fluorescent materials.

### Conclusions

In summary, the introduction of a double-betaine-containing ligand into the lanthanide-POMs reaction system results in the new POM-templated lanthanide-organic hybrid layers with 6<sup>3</sup>-

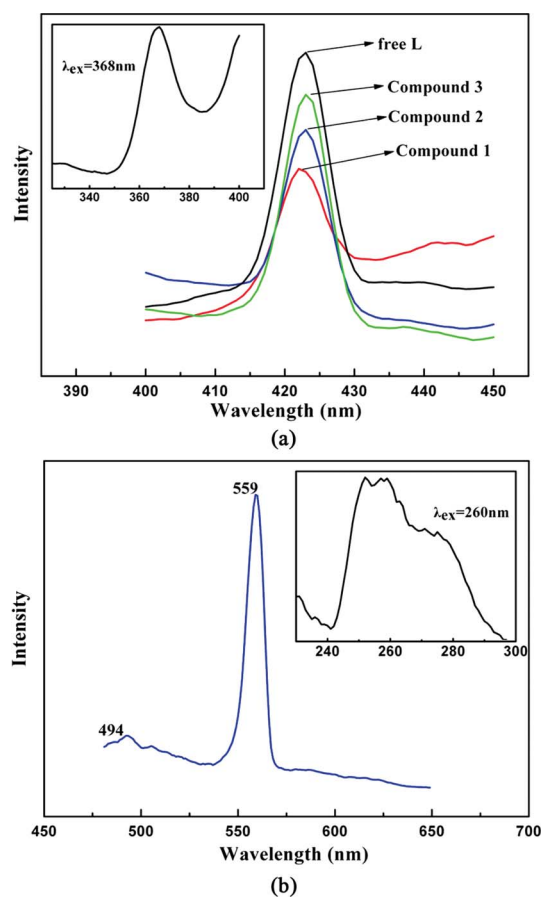


**Fig. 5** (a) Emission spectra of free L (black), compound **1** (red), **2** (blue) and **3** (green) excited at 368 nm. (b) The characteristic luminescence spectrum of Tb(III) in compound **2** excited at 260 nm.

honeycomb-like nets. Based on the present work, it can be expected that the design and use of new double or multiple betaine-containing ligands and/or other POM templates in such reaction systems can assemble more new types of POM-based lanthanide-organic hybrid materials with multifunctional properties in luminescence, electrochemistry, magnetism and catalysis. This work is ongoing in our group.

### References

- (a) M. Eddaoudi, J. Kim, N. Rosi, D. Vodak, J. Wachter, M. O’Keeffe and O. M. Yaghi, *Science*, 2002, **295**, 469; (b) R. Matsuda, R. Kitaura, S. Kitagawa, Y. Kubota, R. V. Belosludov, T. C. Kobayashi, H. Sakamoto, T. Chiba, M. Takata, Y. Kawazoe and Y. Mita, *Nature*, 2005, **436**, 238; (c) R. Banerjee, A. Phan, B. Wang, C. Knobler, H. Furukawa, M. O’Keeffe and O. M. Yaghi, *Science*, 2008, **319**, 939; (d) J. J. Perry IV, J. A. Perman, J. Michael and M. J. Zaworotko, *Chem. Soc. Rev.*, 2009, **38**, 1400; (e) X.-M. Zhang, Z.-M. Hao, W.-X. Zhang and X.-M. Chen, *Angew. Chem., Int. Ed.*, 2007, **46**, 3456; (f) H.-L. Guo, G.-S. Zhu, Ian J. Hewitt and S.-L. Qiu, *J. Am. Chem. Soc.*, 2009, **131**, 1646; (g) X.-L. Wang, C. Qin, S.-X. Wu, K.-Z. Shao, Y.-Q. Lan, S. Wang, D.-X. Zhu, Z.-M. Su and E.-B. Wang, *Angew. Chem., Int. Ed.*, 2009, **48**, 5291.
- (a) A. K. Cheetham, G. Férey and T. Loiseau, *Angew. Chem., Int. Ed.*, 1999, **38**, 3268; (b) J. H. Yu and R. R. Xu, *Acc. Chem. Res.*, 2003, **36**, 481; (c) Y. Song, J. Yu, Y. Li, G. Li and R. Xu, *Angew. Chem., Int. Ed.*, 2004, **43**, 2399.
- (a) P. J. Hagrman, D. Hagrman and J. Zubietta, *Angew. Chem., Int. Ed.*, 1999, **38**, 2638; (b) R. Vilar, D. M. P. Mingos, A. J. P. White and D. J. Williams, *Angew. Chem., Int. Ed.*, 1998, **37**, 1258; (c) L. C. Tabares, J. A. R. Navarro and J. M. Salas, *J. Am. Chem. Soc.*, 2001, **123**, 383.

- 4 (a) M. T. Pope, *Heteropoly and Isopoly Oxometalates*, Springer, Berlin, 1983; (b) M. T. Pope and A. Müller, *Polyoxometalates: From Platonic Solids to Anti-Retroviral 414 Activity*, Kluwer, Dordrecht, 1993; (c) C. L. Hill, *Chem. Rev.*, 1998, **98**, 1, Ed. Special Issue on Polyoxometalates; (d) T. Yamase and M. T. Pope, *Polyoxometalate Chemistry for Nano-Composite Design*, Kluwer, Dordrecht, 2002; (e) D.-L. Long, E. Burkholder and L. Cronin, *Chem. Soc. Rev.*, 2007, **36**, 105; (f) A. Dolbecq, E. Dumas, C. R. Mayer and P. Mialane, *Chem. Rev.*, 2010, **110**, 6009.
- 5 (a) C. Inman, J. M. Knaust and S. W. Keller, *Chem. Commun.*, 2002, 156; (b) L. Lisnard, A. Dolbecq, P. Mialane, J. Marrot, E. Codjovi and F. Sécheresse, *Dalton Trans.*, 2005, 3913; (c) X.-J. Kong, Y.-P. Ren, P.-Q. Zheng, Y.-X. Long, L.-S. Long, R.-B. Huang and L.-S. Zheng, *Inorg. Chem.*, 2006, **45**, 10702; (d) A.-X. Tian, J. Ying, J. Peng, J.-Q. Sha, H.-J. Pang, P.-P. Zhang, Y. Chen, M. Zhu and Z.-M. Su, *Inorg. Chem.*, 2009, **48**, 100; (e) X.-L. Wang, C. Qin, E.-B. Wang and Z.-M. Su, *Chem. Commun.*, 2007, 4245; (f) H.-J. Pang, J. Peng, C.-J. Zhang, Y.-G. Li, P.-P. Zhang, H.-Y. Ma and Z.-M. Su, *Chem. Commun.*, 2010, **46**, 5097; (g) S.-T. Zheng and G.-Y. Yang, *Dalton Trans.*, 2010, **39**, 700.
- 6 (a) L. M. Rodriguez-Albelo, A. R. Ruiz-Salvador, A. Sampieri, D. W. Lewis, A. Gómez, B. Nohra, P. Mialane, J. Marrot, F. Sécheresse, C. Mellot-Draznieks, R. N. Biboum, B. Keita, L. Nadjo and A. Dolbecq, *J. Am. Chem. Soc.*, 2009, **131**, 16078; (b) X.-L. Wang, Y.-F. Bi, B.-K. Chen, H.-Y. Lin and G.-C. Liu, *Inorg. Chem.*, 2008, **47**, 2442; (c) X.-Y. Zhao, D.-D. Liang, S.-X. Liu, C.-Y. Sun, R.-G. Cao, C.-Y. Gao, Y.-H. Ren and Z.-M. Su, *Inorg. Chem.*, 2008, **47**, 7133.
- 7 (a) Y.-G. Li, L.-M. Dai, Y.-H. Wang, X.-L. Wang, E.-B. Wang, Z.-M. Su and L. Xu, *Chem. Commun.*, 2007, 2593; (b) L.-M. Dai, W.-S. You, Y.-G. Li, E.-B. Wang and C.-Y. Huang, *Chem. Commun.*, 2009, 2721.
- 8 (a) M.-L. Wei, C. He, W.-J. Hua, C.-Y. Duan, S.-H. Li and Q.-J. Meng, *J. Am. Chem. Soc.*, 2006, **128**, 13318; (b) C.-Y. Sun, S.-X. Liu, D.-D. Liang, K.-Z. Shao, Y.-H. Ren and Z.-M. Su, *J. Am. Chem. Soc.*, 2009, **131**, 1883; (c) A. Dolbecq, P. Mialane, L. Lisnard, J. Marrot and F. Sécheresse, *Chem.-Eur. J.*, 2003, **9**, 2914.
- 9 (a) M.-L. Wei, C. He, Q.-Z. Sun, Q.-J. Meng and C.-D. Duan, *Inorg. Chem.*, 2007, **46**, 5957; (b) C.-H. Li, K.-L. Huang, Y.-N. Chi, X. Liu, Z.-G. Han, L. Shen and C.-W. Hu, *Inorg. Chem.*, 2009, **48**, 2010; (c) X.-D. Yang, C.-H. Zhang, D.-P. Wang and Y.-G. Chen, *Inorg. Chem. Commun.*, 2010, **13**, 1350; (d) X.-L. Wang, Y.-Q. Guo, Y.-G. Li, E.-B. Wang, C.-W. Hu and N.-H. Hu, *Inorg. Chem.*, 2003, **42**, 4135.
- 10 (a) C. Boglio, G. Lemièrre, B. Hasenknopf, S. Thorimbert, E. Lacote and M. Malacria, *Angew. Chem., Int. Ed.*, 2006, **45**, 3324; (b) N. Dupré, P. Rémy, K. Micoine, C. Boglio, S. Thorimbert, E. Lacôte, B. Hasenknopf and M. Malacria, *Chem. Eur. J.*, 2010, **16**, 7256; (c) Y. Kikukawa, S. Yamaguchi, Y. Nakagawa, K. Uehara, S. Uchida, K. Yamaguchi and N. Mizuno, *J. Am. Chem. Soc.*, 2008, **130**, 15872.
- 11 C.-D. Wu, C.-Z. Lu, H.-H. Zhuang and J.-S. Huang, *J. Am. Chem. Soc.*, 2002, **124**, 3836.
- 12 (a) H.-Y. An, Z.-B. Han and T.-Q. Xu, *Inorg. Chem.*, 2010, **49**, 11403; (b) J. Lü, E.-H. Shen, Y.-G. Li, D.-R. Xiao, E.-B. Wang and L. Xu, *Cryst. Growth Des.*, 2005, **5**, 65.
- 13 (a) D.-D. Wu and T. C. W. Mak, *J. Chem. Soc., Dalton Trans.*, 1995, 139; (b) J.-G. Mao, H.-J. Zhang, J.-Z. Ni, S.-B. Wang and T. C. W. Mak, *Polyhedron*, 1999, **18**, 1519; (c) X. Zhang, G.-C. Guo, F.-K. Zheng, G.-W. J.-G. Zhou, Z.-C. Dong, J.-S. Huang and T. C. W. Mak, *J. Chem. Soc., Dalton Trans.*, 2002, 1344; (d) A.-Q. Wu, Y. Li, F.-K. Zheng, G.-C. Guo and J.-S. Huang, *Cryst. Growth Des.*, 2006, **6**, 444.
- 14 R. D. Claude, F. Michel, F. Raymonde and T. Rene, *Inorg. Chem.*, 1983, **22**, 207.
- 15 F.-K. Zheng, A.-Q. Wu, Y. Li, G.-C. Guo and J.-S. Huang, *Chin. J. Struct. Chem.*, 2005, **24**, 940.
- 16 (a) G. M. Sheldrick, *SHELXL97*, Program for Crystal Structure Refinement, University of Göttingen, Göttingen, Germany, 1997; (b) G. M. Sheldrick, *SHELXS97*, Program for Crystal Structure Solution, University of Göttingen, Göttingen, Germany, 1997.
- 17 M. Sadakane and E. Stechhan, *Chem. Rev.*, 1998, **98**, 219.
- 18 S. Don, X. Xi and M. Tian, *J. Electroanal. Chem.*, 1995, **385**, 227.
- 19 K. Unoura and N. Tanaka, *Inorg. Chem.*, 1983, **22**, 2963.
- 20 (a) X.-L. Wang, Z.-H. Kang, E.-B. Wang and C.-W. Hu, *J. Electroanal. Chem.*, 2002, **523**, 142; (b) L. Cheng, X.-M. Zhang, X.-D. Xi and S.-J. Dong, *J. Electroanal. Chem.*, 1996, **407**, 97.
- 21 B. Zhao, X.-Y. Chen, P. Cheng, D.-Z. Liao, S.-P. Yan and Z.-H. Jiang, *J. Am. Chem. Soc.*, 2004, **126**, 15394.
- 22 (a) F.-Y. Yi, N. Zhao, W. Wu and J.-G. Mao, *Inorg. Chem.*, 2009, **48**, 628; (b) X.-X. Zhou, Y.-P. Cai, S.-Z. Zhu, Q.-G. Zhan, M.-S. Liu, Z.-Y. Zhou and L. Chen, *Cryst. Growth Des.*, 2008, **8**, 2076; (c) B. Xu, J. Lü and R. Cao, *Cryst. Growth Des.*, 2009, **9**, 3003.
- 23 W.-K. Wong, X.-P. Yang, Richard A. Jones, Joseph H. Rivers, Vince Lynch, Wing-Kit Lo, D. Xiao, Michael M. Oye and Archie L. Holmes, *Inorg. Chem.*, 2006, **45**, 4340.